

# Photocurrent Response from Vertically Aligned Single-walled Carbon Nanotube Arrays

Mark Bissett<sup>1</sup>, Ingo Koper<sup>1</sup>, Joe Shapter<sup>1</sup>

<sup>1</sup>School of Chemical and Physical Sciences, Flinders University  
Bedford Park, South Australia, 5042 Australia

**Abstract**— Vertically-aligned arrays of single walled carbon nanotubes were created on an optically transparent electrode (FTO glass) these arrays were found to exhibit a prompt current and voltage when exposed to light. These cells were then investigated by electrochemical impedance spectroscopy and found to exhibit a dampening of the recombination reaction over the first 24 hours. Symmetrical cell modeling was successful in simulating the behavior of normal cell architecture.

**Keywords;** carbon nanotubes, SWCNT, EIS, solar cell

## I. INTRODUCTION

Single walled carbon nanotubes (SWCNT) are unique materials that provide many interesting possibilities for device architecture. As well as having many interesting material properties, such as high tensile strength and Young's modulus, they also possess high electrical conductivity and a rich density of states that allows them to form both conductors and semi-conductors [1]. Recently there has been a large degree of interest in solar cell design and cell architecture, specifically the advent of the dye-sensitized solar cell (DSSC) [2-4]. DSSCs work on a simple design that utilises a kind of artificial photosynthesis. A  $\text{TiO}_2$  layer is placed on a transparent conductive substrate (usually ITO or FTO coated glass). Onto this layer a photosensitive dye is attached, and the cell is constructed by sandwiching this working electrode between an electrolyte and a platinum coated counter electrode. The electrolyte used is typically an iodide/tri-iodide ( $\text{I}^-/\text{I}_3^-$ ) redox couple, the thin platinum layer acts as a redox catalyst greatly enhancing the cell performance [5]. SWCNT can be of benefit in several ways. Firstly there has been some evidence that carbon nanotubes can replace platinum as a catalyst because of their high surface area and electronic properties [6-8]. However, these SWCNTs are also of interest because they can also act as photosensitive elements themselves [9-12]. Light response of the cell is measured by measuring current-voltage response (I-V curves) under illumination. Also of interest to researchers is the behavior inside the DSSCs and at interfaces between each element. This can be elucidated by electrochemical impedance spectroscopy (EIS) [13-15]. The cell design shown in Figure 1 replaces the dye-sensitized  $\text{TiO}_2$  with an array of vertically aligned SWCNT that is chemically attached to FTO coated glass by a technique previously performed extensively in our research group [16-20].

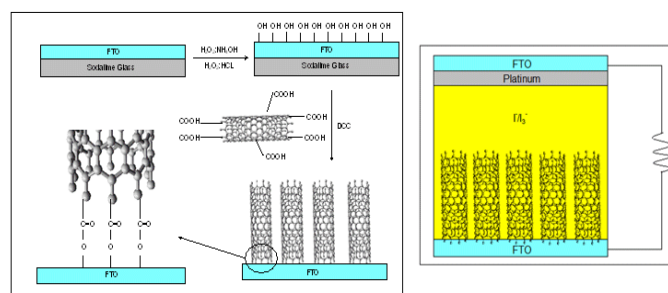


Figure 1: CNT attachment Schematic and Cell Design Schematic

This array of SWCNT behaves as a semi-conductor due to chemical treatment and can generate electron-hole pairs when exposed to visible light. Cells were constructed to investigate the response to visible light and a prompt current response was found. Symmetrical cells, cells made from either a counter-counter electrode pair or working-working electrode pair were produced and modeled using EIS. These structures were used to simulate the behavior in normal counter-working electrode cells. This allowed for a much greater understanding of the internal mechanism within the cell.

## II. EXPERIMENTAL

### A. Single Walled Carbon Nanotube Arrays

Carbon nanotube arrays were prepared by modifying an existing technique [18]. It is outlined here in brief. Purified low functionality single walled carbon nanotubes (P2-SWCNT, Carbon Solutions, Inc.) were purchased and sonicated at  $0^\circ\text{C}$  in a 3:1 (v/v) mixture of  $\text{H}_2\text{SO}_4:\text{HNO}_3$  for 8 hours. This acid treatment does several things; shortens the nanotubes, dissolves catalyst particles, removes amorphous carbon and introduces carboxylic acid groups to defect sites along the tube walls and ends. The resulting functionalized nanotube solution was then filtered through a  $0.4\mu\text{m}$  membrane (Isopore HTTP, Millipore) and dispersed in dimethyl sulfoxide (DMSO) at  $0.2\text{mg/ml}$ . Dicyclohexyl carbodiimide (DCC) was added at 1:1 (w/w) of cut nanotube and the solution was stored under nitrogen in a glove box. Fluorine doped tin oxide glass (TCO22-15, Solaronix SA,  $15\ \Omega/\text{square}$ ) was hydroxylated by first treating with  $\text{H}_2\text{O}_2$  and  $\text{NH}_4\text{OH}$  and then with  $\text{H}_2\text{O}_2$  and  $\text{HCl}$ . The hydroxylated FTO glass substrates were then submerged in the SWCNT solution

and stored at 80°C for 24 hours. The aligned nanotube arrays were rinsed with acetone and dried with nitrogen before being used.

### B. Solar Cell Preparation

Electrochemical solar cells were constructed by using the SWNT modified FTO glass as the working electrode while counter electrodes were produced by taking FTO glass with fill holes already in place and sputtering a 10nm platinum coating to act as a catalyst. Gaskets were made from 60µm thick Surlyn® (SX1170-60, Solaronix SA) sandwiched between the counter and working electrodes and heated to 100°C in an oven for 10 minutes. The cell was then filled with a solution of 0.8M 1-methyl-3-propylimidazolium iodide (Sigma-Aldrich), 0.1M iodine (Sigma-Aldrich) and 0.3M benzimidazole (Sigma-Aldrich) in 3-methoxypropylamine (Sigma-Aldrich), to make an iodide/tri-iodide ( $I/I_3^-$ ) redox couple. The fill hole was then sealed with more Surlyn® and a glass microscope cover slip.

### C. Photoresponse

I-V measurements were taken using a Keithley 2400 Source-Measure unit interfaced with Labview based software written in-house. Measurements were taken under illumination from an optic fibre light source (Dolan-Jenner Fiber-Lite 190-1) at  $\sim 35\text{mW/cm}^2$ , measured with a light meter (Newport Power Meter, Model 1815-C).

### D. Electrochemical Impedance Spectroscopy

Frequency response was performed using an Ecochemie microAutolab Type III/FRA2 on both normal and symmetrical cells. Counter-counter cells were analyzed in the dark and working-working and plain cells were analyzed under illumination by an optic fibre light source (Dolan-Jenner Fiber-Lite 190-1) at  $\sim 35\text{mW/cm}^2$  at 0mV bias. The amplitude of the perturbation signal was 10mV and the frequency range was logarithmically distributed from 0.02-10000Hz. Fitting was performed using the frequency response analyser software packaged with the microAutolab (FRA version 4.9).

## III. RESULTS AND DISCUSSION

To first investigate the response of the normal cell to visible light the current was measured as the light source was switched on and off. This can be used to determine the response time of the cell which was found to be of approximately 200ms and to a maximum current of  $4.5\mu\text{A/cm}^2$  (Fig. 2a). Light soaking experiments showed that the current remains constant over a prolonged period of time.

To further investigate the photoresponse of the cells I-V curves were taken under illumination. Of note was that the cells were tested immediately after preparation and then again each 24Hrs to check for long term performance. However, the difference in cell behavior between the fresh and day old sample was much larger than expected and then remained constant after the first 24Hrs. This can be seen in the I-V curves in fig. 2b. The I-V curves seen are fairly linear with a fill factor of around 30%; this is attributed to a very low shunt

resistance in the SWCNT-electrolyte interface allowing for a large back reaction or recombination to occur.

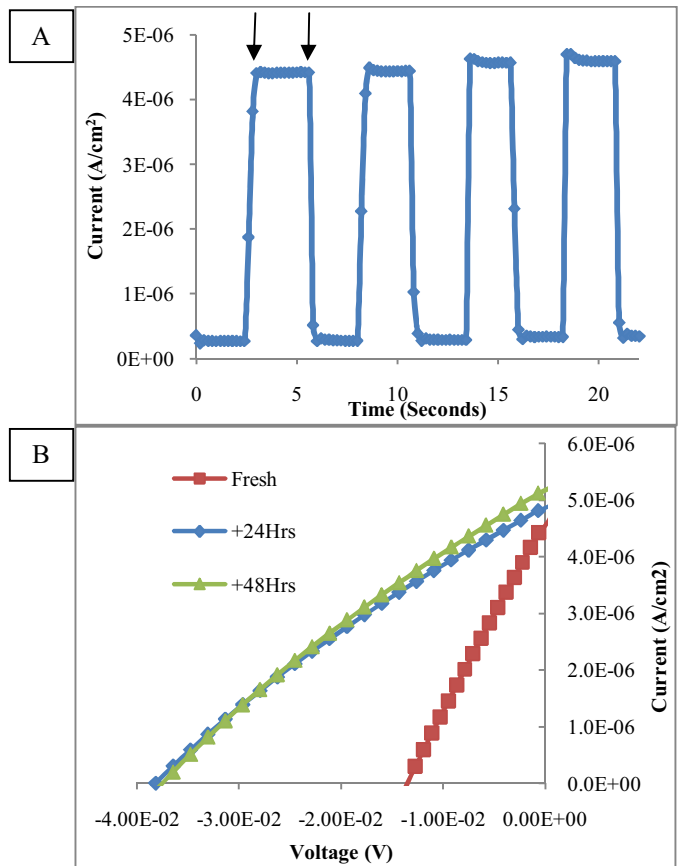


Figure 2: (A) Light response from FTO-CNT cell. Arrows indicating the light on and off cycle. (B) I-V curve for plain cell under illumination for a freshly prepared and aged cell.

To investigate this ageing affect as well as the back reaction EIS spectra were taken of a freshly prepared and aged cell. Typically the Nyquist plot of a  $\text{TiO}_2$  DSSC shows three semi-circles. The first, in order of decreasing frequency, is due to the Pt-FTO interface, the second the  $\text{TiO}_2$ -electrolyte interface and lastly the Nernst diffusion of the ions in the electrolyte [14, 21]. The Nyquist plot of the SWCNT-cell after being freshly prepared and also aged by 24 and 48 hours is shown in fig. 3a. Clearly there is a noticeable correlation between the EIS spectra and the I-V curves indicating that there is a definite change in the cell behavior over the first 24 hours that then remains constant. This change is seen to cause both the current and voltage to increase, whilst the impedance of the SWCNT-electrolyte interface has increased. To better understand this phenomenon we must look at the Bode plot in fig. 3b. When we compare the peak shift after ageing the central peak has shifted to a lower frequency, see table 1. We can convert these frequencies into the effective electron lifetime ( $\tau_{\text{eff}}$ ) by using the equation given in [21]. The much longer electron lifetime in the aged cell indicates that the recombination process that can occur between the SWCNT-electrolyte interfaces has been suppressed. This reduced recombination is also the reason for the increase in

photocurrent and voltage seen in the I-V curves in fig. 2b. The physical process behind this “ageing” effect is believed to be related to the formation of the electric double layer in the electrolyte. Interestingly this increase in  $\tau_{\text{eff}}$  is the opposite effect seen in TiO<sub>2</sub> cells which see a shift to higher frequency caused by degradation of the mesoporous layer, suggesting that the nanotube array possesses an excellent stability [21].

**Table 1: Frequency ( $f$ ) and effective electron lifetime ( $\tau_{\text{eff}}$ ) for fresh and aged cells**

Cell type	$f$ (Hz)	$\tau_{\text{eff}}$ (ms)
Fresh	9.824	16.20
Aged +24Hrs	3.821	41.65
Aged +48Hrs	3.821	41.65

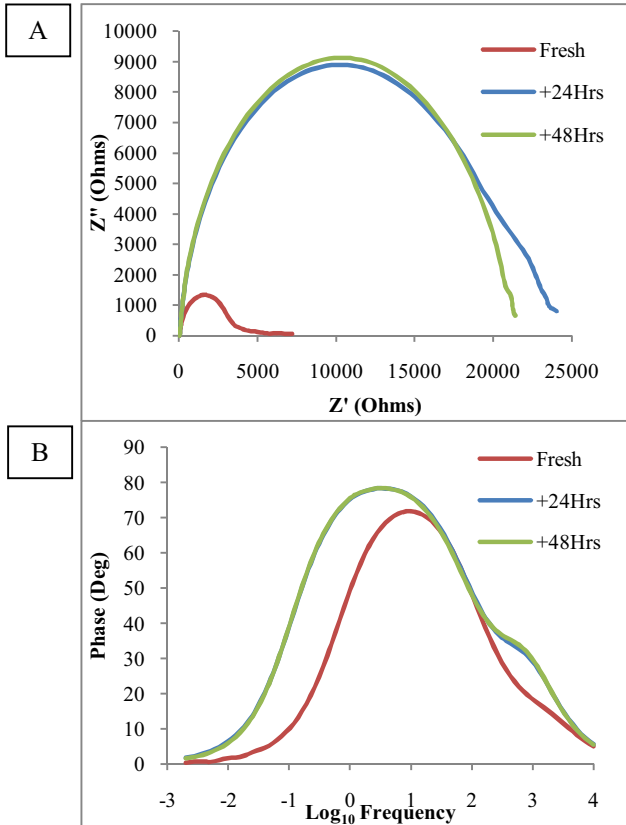


**Figure 3: Nyquist plot (A) and Bode plot (B) (without illumination) for a freshly prepared and aged plain cell. Cells were stored in the dark between testing.**

Symmetrical cells were created from both the counter electrode (Pt-Pt) and working electrode (SWCNT-SWCNT). This allows us to exclude the effect of one electrode and simplifies the spectra for fitting. In a platinum counter-counter symmetrical cell we expect to see two peaks, the first is attributed to charge transfer at the Pt/FTO interface whilst the second is ionic diffusion in the electrolyte [15]. This is observed in the measured data of fig. 4a.

The second semi-circle attributed to ionic diffusion will be excluded from fitting to simplify the equivalent cell. In the working electrode symmetrical cell we expect again two semi-circles; the first is now attributed to effective electron lifetime in the nanotubes and the second, again the ionic diffusion. In the case of the measured data in fig. 4b we see the first

semicircle but the low frequency Nernst diffusion is obstructed by noise and thus will be excluded from fitting. The equivalent circuit for the normal cell to be used is simply a series resistance connected to two Randles type circuits and is shown in fig. 4c. When fitting a symmetrical cell we can take  $R_2=R_3$  and  $CPE1=CPE2$  and simplify to a single Randles type circuit and a series resistance.

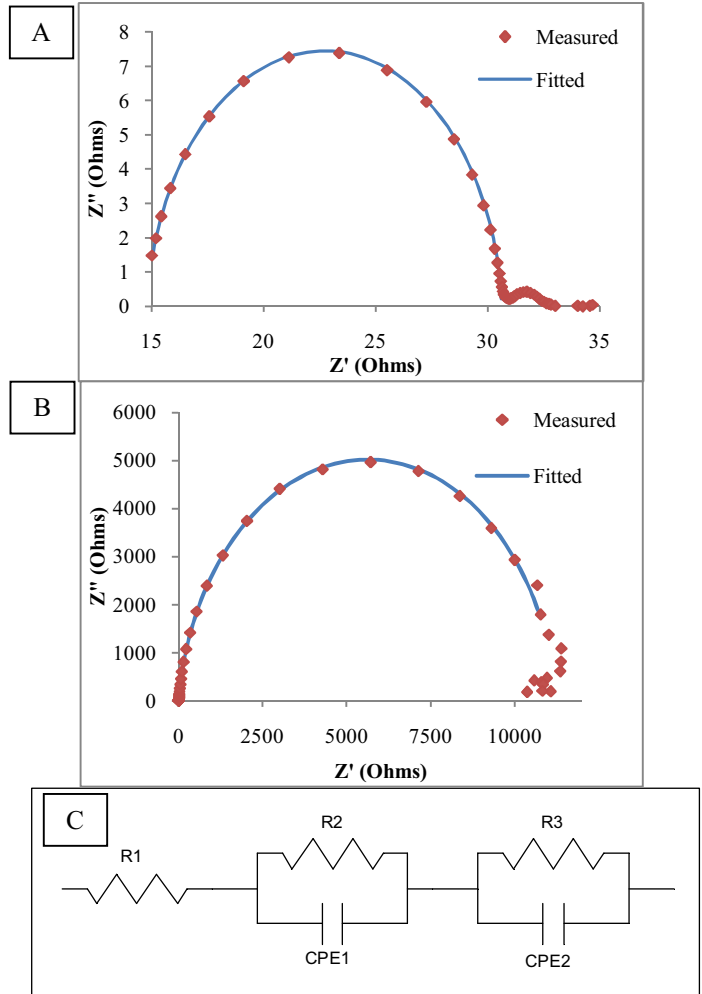


**Figure 4: Pt Symmetrical cell in dark (A) SWCNT Symmetrical cell in light (B) Equivalent circuit used for fitting (C)**

By fitting the equivalent circuit in fig. 4c to the data from the symmetrical cells we can then combine the two together into the normal cell and predict its behavior. That simulation and the comparison to the measured normal cell is shown in fig. 5. It can be seen that the data matches quite closely to that of the simulation indicating that the equivalent circuit proposed does indeed match, and that the technique of using the counter and working electrode symmetrical cells can be used to predict behavior in normal cells. The mismatch between the two is due to the simplicity of the model used.

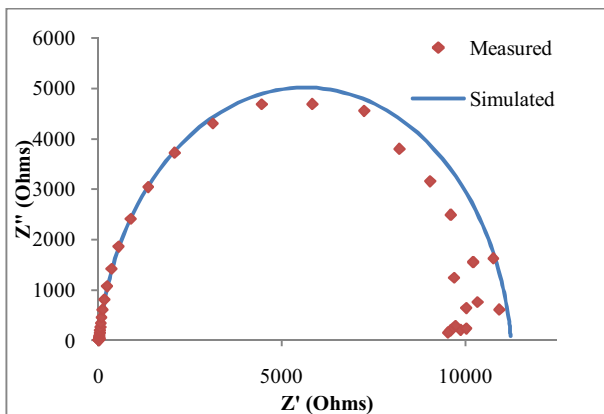


Figure 5: Normal cell Nyquist plot for both measured and simulated data using symmetrical cells.

#### IV. CONCLUSION

Vertically-aligned single walled carbon nanotube arrays were created on FTO glass. These arrays were found to exhibit a prompt and stable photoresponse, giving a current of approx.  $5\mu\text{A}/\text{cm}^2$  for a  $35\text{mW}/\text{cm}^2$  light. These cells were then examined using EIS and it was possible to model and predict cell behavior based on these models. Interestingly the cells were found to increase in response due to ageing and this was caused by an increased effective electron lifetime in the conduction band of the carbon nanotubes. It is suggested that this is caused by the time taken for the electric double layer to be formed in the electrolyte at the SWCNT-electrolyte interface.

#### REFERENCES

- [1] R. Saito, G. Dresselhaus, and M. S. Dresselhaus, *Physical Properties of Carbon Nanotubes*. London: Imperial College Press, 1998.
- [2] B. Oregan and M. Gratzel, "A LOW-COST, HIGH-EFFICIENCY SOLAR-CELL BASED ON DYE-SENSITIZED COLLOIDAL TiO<sub>2</sub> FILMS," *Nature*, vol. 353, pp. 737-740, Oct 1991.
- [3] M. Gratzel, "Photoelectrochemical cells," *Nature*, vol. 414, pp. 338-344, 2001.
- [4] M. Gratzel, "Dye-sensitized solar cells," *Journal of Photochemistry and Photobiology C-Photochemistry Reviews*, vol. 4, pp. 145-153, Oct 2003.
- [5] A. Hauch and A. Georg, "Diffusion in the electrolyte and charge-transfer reaction at the platinum electrode in dye-sensitized solar cells," *Electrochimica Acta*, vol. 46, pp. 3457-3466, 2001.
- [6] K. Suzuki, M. Yamaguchi, M. Kumagai, and S. Yanagida, "Application of Carbon Nanotubes to Counter Electrodes of Dye-sensitized Solar Cells," *Chemistry Letters*, vol. 32, pp. 28-29, 2003.
- [7] E. Ramasamy, W. J. Lee, D. Y. Lee, and J. S. Song, "Spray coated multi-wall carbon nanotube counter electrode for tri-iodide reduction in dye-sensitized solar cells," *Electrochemistry Communications*, vol. 10, pp. 1087-1089, 2008.
- [8] C.-S. Chou, R.-Y. Yang, M.-H. Weng, and C.-I. Huang, "The applicability of SWCNT on the counter electrode for the dye-sensitized solar cell," *Advanced Powder Technology*, vol. 20, pp. 310-317, 2009.
- [9] S. Barazzouk, S. Hotchandani, K. Vinodgopal, and P. V. Kamat, "Single-Wall Carbon Nanotube Films for Photocurrent Generation. A Prompt Response to Visible-Light Irradiation," *J. Phys. Chem. B*, vol. 108, pp. 17015-17018, 2004.
- [10] P. Castrucci, F. Tombolini, M. Scarselli, E. Speiser, S. D. Gobbo, W. Richter, M. D. Crescenzi, M. Diociaiuti, E. Gatto, and M. Venanzi, "Large photocurrent generation in multiwall carbon nanotubes," *Applied Physics Letters*, vol. 89, p. 253107, 2006.
- [11] P. V. Kamat, "Harvesting photons with carbon nanotubes," *Nano Today*, vol. 1, pp. 20-27, 2006.
- [12] Z. Li, V. P. Kunets, V. Saini, Y. Xu, E. Dervishi, G. J. Salamo, A. R. Biris, and A. S. Biris, "Light-Harvesting Using High Density p-type Single Wall Carbon Nanotube/n-type Silicon Heterojunctions," *ACS Nano*, vol. 3, pp. 1407-1414, 2009.
- [13] J. van de Lagemaat, N. G. Park, and A. J. Frank, "Influence of Electrical Potential Distribution, Charge Transport, and Recombination on the Photopotential and Photocurrent Conversion Efficiency of Dye-Sensitized Nanocrystalline TiO<sub>2</sub> Solar Cells: A Study by Electrical Impedance and Optical Modulation Techniques," *The Journal of Physical Chemistry B*, vol. 104, pp. 2044-2052, 2000.
- [14] Q. Wang, J. E. Moser, and M. Gratzel, "Electrochemical Impedance Spectroscopic Analysis of Dye-Sensitized Solar Cells," *J. Phys. Chem. B*, vol. 109, pp. 14945-14953, 2005.
- [15] M. Liberatore, F. Decker, L. Burtone, V. Zardetto, T. Brown, A. Reale, and A. Di Carlo, "Using EIS for diagnosis of dye-sensitized solar cells performance," *Journal of Applied Electrochemistry*, vol. 39, pp. 2291-2295, 2009.
- [16] B. S. Flavel, J. Yu, J. G. Shapter, and J. S. Quinton, "Patterned attachment of carbon nanotubes to silane modified silicon," *Carbon*, vol. 45, pp. 2551-2558, 2007.
- [17] J. Yu, B. S. Flavel, and J. G. Shapter, "Optical and electrochemical properties of single-walled carbon nanotube arrays attached to silicon(100) surfaces," *Fullerenes Nanotubes and Carbon Nanostructures*, vol. 16, pp. 18-29, 2008.
- [18] J. X. Yu, D. Losic, M. Marshall, T. Bocking, J. J. Gooding, and J. G. Shapter, "Preparation and characterisation of an aligned carbon nanotube array on the silicon (100) surface," *Soft Matter*, vol. 2, pp. 1081-1088, Dec 2006.
- [19] B. S. Flavel, J. X. Yu, J. G. Shapter, and J. S. Quinton, "Patterned ferrocenemethanol modified carbon nanotube electrodes on silane modified silicon," *Journal of Materials Chemistry*, vol. 17, pp. 4757-4761, 2007.
- [20] J. X. Yu, J. G. Shapter, J. S. Quinton, M. R. Johnston, and D. A. Beattie, "Direct attachment of well-aligned single-walled carbon nanotube architectures to silicon (100) surfaces: a simple approach for device assembly," *Physical Chemistry Chemical Physics*, vol. 9, pp. 510-520, 2007.
- [21] R. Kern, R. Sastrawan, J. Ferber, R. Stangl, and J. Luther, "Modeling and interpretation of electrical impedance spectra of dye solar cells operated under open-circuit conditions," *Electrochimica Acta*, vol. 47, pp. 4213-4225, 2002.